

# A Computational Intelligence Approach to Mobile Network Coverage Determination across a typical Guinea Savanna Belt Rural Terrain

**Deme C. Abraham**

Department of Computer Science,  
University of Jos, Nigeria.  
demeabraham@gmail.com, acdeme2000@yahoo.com

**Abstract**—This study proposes a computational intelligence approach to field strength estimation across a typical Guinea Savanna Belt rural terrain. The three networks considered were the Radial Basis Function Neural Network (RBF-NN), the Adaptive Neuro-Fuzzy Inference System (ANFIS), and the Multilayer Perceptron Neural Network (MLP-NN). Prediction models based on these networks were created, trained and tested for field strength prediction using received power signals recorded at an operating frequency of 1800MHz, from multiple Base Transceiver Stations (BTS) situated within the rural terrain between Bauchi City and Darazo town, in Northern Nigeria. Results indicate that the three computational networks can predict with an average Root Mean Squared Error (RMSE) value less than 5dBm. However, the RBF-NN based predictor gave the highest prediction accuracy with a RMSE value of 4.67dBm.

**Keywords**—Field Strength; COST 231 Hata; GRBFNN, ANFIS, MLPNN

## I. INTRODUCTION

Network coverage prediction is of paramount importance in wireless network planning. Over the years, numerous techniques have been implemented in order to proffer greater prediction accuracy. Such techniques include the use of Deterministic Models, which widely used techniques for signal strength prediction. As described in [1], Deterministic Models make use of the laws governing electromagnetic wave propagation to determine the received signal power at a particular location. The field strength is calculated using the Geometrical Theory of Diffraction (GTD) as a component comprising of direct, reflected and diffracted rays at the required position. Deterministic models often require a complete 3-D map of the propagation environment. The ray tracing model used by [2] in radio propagation modeling is a typical example of

deterministic models. Recent approaches to field strength prediction are based on computational intelligence as clearly documented in [3], [4].

Computational intelligence methods are quite efficient in handling problems associated with uncertainty, imprecision, approximation, etc. Hence, they are useful in finding acceptable solutions to complex real world problems such as pattern recognition, speech processing, function approximation, signal processing, forecasting, etc. Such methods include artificial neural networks, genetic algorithms, fuzzy sets, neuro-fuzzy systems, etc.

The problem of field strength prediction is viewed as a function approximation problem consisting of a nonlinear mapping from a set of input variables containing information about the potential receiver onto a single output variable representing the predicted field strength [3]. Hence, the study is aimed at exploring the remarkable abilities of Computational intelligence methods to handle such tasks.

This paper presents computational intelligence based models for field strength determination across a typical Guinea Savanna Vegetation Belt rural terrain. The Nigerian Guinea Savanna Vegetation Belt is essentially a woodland comprising of a mixture of trees and tall grasses. The terrain under investigation is a thinly rural terrain between the city of Jos and Keffi town, comprising of scattered houses and trees above 6 meters.

The computational intelligence predictors considered are based on the Radial Basis Function Neural Network (RBF-NN), the Adaptive Neuro-Fuzzy Inference System (ANFIS) and Multilayer Perceptron Neural Network (MLP-NN). These predictors along with the COST 231 Hata model are statistically compared for prediction accuracy using received power values recorded at an operating frequency of 1800MHz, from multiple Base Transceiver Stations (BTS) within terrain.

## II. THE GENERALIZED RADIAL BASIS FUNCTION NEURAL NETWORK

The generalized Radial Basis Function Neural Network (RBF-NN) can be used to solve problems that demand the implementation of function approximation. The generalization is equivalent to the use of this multi-dimensional surface to interpolate the test data.

As described in [5], RBF networks have three layers: input layer, hidden layer and output layer. One neuron in the input layer corresponds to each predictor variable. With respects to categorical variables, n-1 neurons are used where n is the number of categories. Hidden layer has a variable number of neurons. Each neuron consists of a radial basis function centered on a point with the same dimensions as the predictor variables. The output layer has a weighted sum of outputs from the hidden layer to form the network outputs.

Unlike the MLP, the output of hidden-nodes are not calculated using the weighted-sum activation function; rather the output of each hidden-node,  $\phi_k$  is obtained by the closeness of input  $X$  to an M-dimensional parameter vector  $\mu_k$  associated with the  $k^{\text{th}}$  hidden node [6]. As shown in Fig. 1, the RBF-NN consists of three layers as follows:

- i. The input layer
- ii. The hidden layer, where input data undergoes nonlinear transformation
- iii. The linear output layer, where the outputs are produced

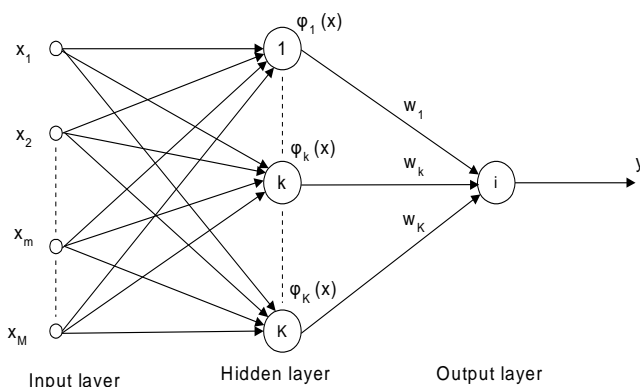


Fig. 1: *The Generalized Radial Basis Function Neural Network [6].*

The most popular choice for the function  $\phi$  is a multivariate Gaussian function with an appropriate mean and auto covariance matrix [6]. The output of a Radial Basis Function Neural Network is given by (1)

$$Y_i(X) = \sum_{k=1}^K w_{ik} \phi_k(X) \quad (1)$$

where,

$X$  is the input vector

$w_{ik}$  is the connection weight in the second layer (from hidden to output layer)

$k$  is the number of hidden nodes

$i$  denotes the  $i$ -th hidden node

$\phi_k$  is the radial basis activation function.

As described in [7], the radial basis function is a multi-dimensional function that describes the distance between a given input vector and a pre-defined centre vector. The Gaussian function is a type of radial basis function given by (2)

$$\phi_k = \exp\left(-\frac{\|X - \mu_k\|^2}{2\sigma_k^2}\right) \quad (2)$$

Where,

$\mu_k$  denotes the center vector

$\sigma_k$  denotes the spread (width) of the function

The learning process is equivalent to finding a surface in a multidimensional space that provides a best fit to the training data, with the criterion for the "best fit" being measured in some statistical sense [6]. The training of a RBFNN is in two stages:

1. Determination of radial basis function parameters, i.e., Gaussian centre and spread width
2. Determination of output weight by supervised learning.

## III. THE ADAPTIVE NEURO-FUZZY INFERENCE SYSTEM

As described in [8], the Adaptive Neuro-Fuzzy Inference System (ANFIS) is a hybrid system comprising of an Artificial Neural Network (ANN) a Fuzzy Inference System (FIS). ANFIS was first proposed by [9] to combine the learning ability of ANNs with the ability of fuzzy systems to interpret imprecise information. ANFIS is an intelligent adaptive system capable of solving complex non-linear problems. The capability of the ANFIS stems from the fact that the ANN part is suitable for modeling systems where there is no mathematical relationship between input and output patterns. Furthermore, as systems that mimic the human brain, ANNs can be trained using input patterns and target output, and then used to predict a result given new set of inputs. On the other hand, FIS is a computational network capable of modeling human knowledge and reasoning, based on the concepts of fuzzy set theory, fuzzy if-then rules, and fuzzy reasoning.

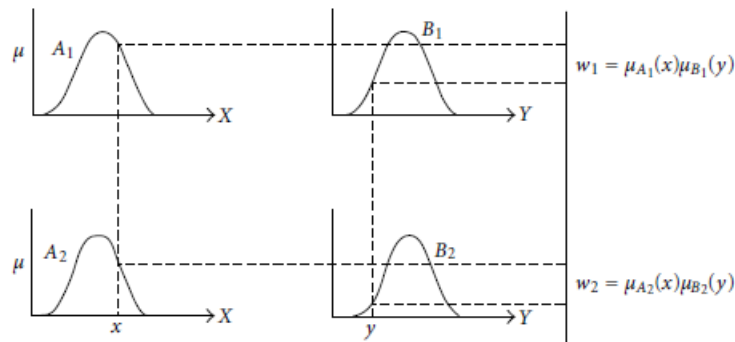


Fig. 2: First Order Sugeno Model [11]

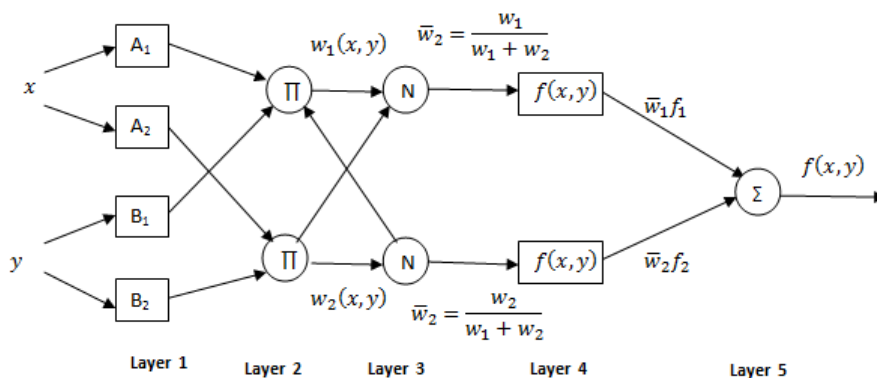


Fig. 3: The Architecture of an Adaptive Neuro-Fuzzy Inference System

The ANFIS model considered in this study is based on the model proposed by [10], referred to as the First Order Sugeno Fuzzy Model (or simply TS Model) shown in Fig. 2. The ANFIS architecture in Fig. 3 is based on the TS model, with two inputs,  $x$  and  $y$  and one output which is a function of the inputs.

Based on the TS Model, the two *if-then-else* rules are as follows:

- i) If ( $x$  is  $A_1$ ) and  $y$  is  $B_1$ , THEN  $f_1 = p_1 x + q_1 y + r_1$
- ii) If ( $x$  is  $A_2$ ) and  $y$  is  $B_2$ , THEN  $f_2 = p_2 x + q_2 y + r_2$

The linguistic labels  $A_i$  and  $B_i$  are fuzzy sets associated with the input nodes  $x$  and  $y$  respectively, and  $f_i$  is a non-fuzzy function which depends on the inputs  $x$  and  $y$ .

As shown in Fig. 3, the ANFIS architecture comprises of five layers and each layer is defined by specific nodes, which can either be fixed or adaptive. A fixed node is denoted by a circle while a square represents an adaptive node.

As described in [4], the architectural layers of an ANFIS are as follows:

**Layer 1 :** In this layer, every node is an adaptive node with a node function given by:

$$O_{1,i} = \mu_{A_i}(x) \text{ for } i = 1,2 \tag{3}$$

$$O_{1,i} = \mu_{B_{i-2}}(y) \text{ for } i = 3,4 \tag{4}$$

These functions are defined by Membership Functions (MF) which can either be Bell, Gaussian or Triangular. The most widely used MF is the Bell MF given by (5):

$$\mu_{A_i}(x) = \frac{1}{1 + \left[ \frac{x - c_i}{a_i} \right]^{2b_i}} \tag{5}$$

**Layer 2:** This layer comprises of fixed nodes and the output of every node is the product of all the incoming signals into the node as given by (6). These node outputs are the firing strengths of the rules.

$$w_i = \mu_{A_i}(x_i) \mu_{B_i}(y_i) \tag{6}$$

**Layer 3:** This layer also comprises of fixed nodes, which are denoted by N. This is the normalization layer where the ratio of the firing strength of each rule

is calculated with respect to the sum of the firing strengths of all rules, using (7). Hence, the outputs of this layer are referred to as normalized firing strengths.

$$\bar{w}_i = \frac{w_i}{\sum_{j=1}^2 w_j} \quad (7)$$

**Layer 4:** The nodes in this layer are adaptive nodes. The output of each node is the product of the normalized firing strength and a first order polynomial (for the first order TS model), given by (8):

$$\bar{w}_i f_i = \bar{w}_i (p_i x + q_i y + r_i) \quad (8)$$

The parameters  $p_i$ ,  $q_i$  and  $r_i$  are called consequent parameters.

**Layer 5:** This is the output layer and it has a single fixed node labeled  $\Sigma$ . The layer computes the overall output as the summation of all incoming signals, to produce a crisp output given by (9):

$$f(x, y) = \sum_i \bar{w}_i f_i = \frac{\sum_i w_i f_i}{\sum_i w_i} \quad (9)$$

According to [12], ANFIS uses a hybrid learning algorithm comprising of gradient descent back-propagation and the least-squares approximation method. During network training the back-propagation algorithm determines the premise parameters while the least-squares approximation method determines the consequent parameters.

#### IV. THE MULTI-LAYER PERCEPTRON NEURAL NETWORK

As described in [13], the Multi-Layer Perceptron Neural Network (MLP-NN) is a multilayer feed forward neural network used for nonlinear function approximation. As the name implies, a MLP-NN is a network that comprises of an input layer, one or more hidden layers and an output layer. However, according to [14], a neural network with only one hidden layer can approximate any function with finitely many discontinuities to an arbitrary precision, provided the activation functions of the hidden units are non-linear.

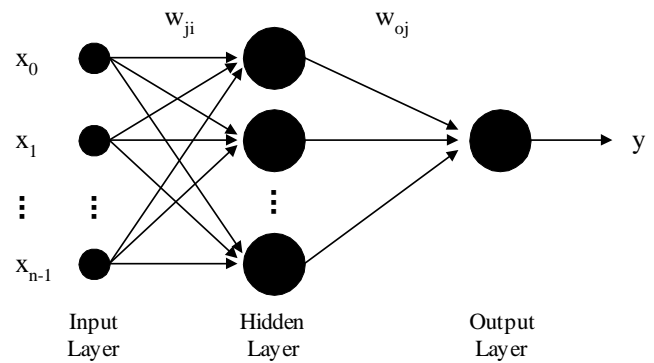


Fig. 4: Multilayer Perceptron Neural Network with one hidden layer [13]

Fig. 4 shows that each neuron of the input layer is connected to each neuron of the hidden layer, and in turn, each neuron of the hidden layer is connected to the single neuron of the output layer. As a result, signal transmission across the entire network can only be in the forward direction, i.e, from the input layer, through the hidden layer and eventually to the output layer. Signals arriving at the inputs propagate forward from neuron to neuron, until they finally arrive at the output neuron and emerge as output signals. Error signals propagate in the opposite direction from the output neuron across the network. The output of the MLP-NN is describe by the following expression (10)

$$y = F_0 \left( \sum_{j=0}^M w_{0j} \left( F_h \left( \sum_{i=0}^N w_{ji} X_i \right) \right) \right) \quad (10)$$

where:

$w_{0j}$  represents the synaptic weights from neuron  $j$  in the hidden layer to the single output neuron

$X_i$  represents the  $i^{\text{th}}$  element of the input vector,

$F_h$  and  $F_0$  are the activation function of the neurons from the hidden layer and output layer,

respectively,

$w_{ji}$  are the connection weights between the neurons of the hidden layer and the inputs.

The learning phase of the network proceeds by adaptively adjusting the free parameters of the system based on the mean squared error  $E$ , described by (11), between predicted and measured path loss for a set of appropriately selected training examples:

$$E = \frac{1}{2} \sum_{i=1}^m (y_i - d_i)^2 \quad (11)$$

Where,  $y_i$  is the output value calculated by the network and  $d_i$  represents the expected output.

When the error between network output and the desired output is minimized, the learning process is terminated and the network can be used in a testing phase with test vectors. At this stage, the neural network is described by the optimal weight configuration, which means that theoretically ensures the output error minimization.

## V. THE COST 231 HATA MODEL

As described in [4], The COST 231 Hata Model is an extension of the Hata, formulated to suit the European environments taking into consideration a wider range of frequencies (500MHz to 200MHz). The Hata model in turn is an extension of the Okumura Model. The Hata model is suitability for path loss prediction in urban, semi-urban, suburban and rural areas, and the model expression is given by (12)

$$L = 46.3 + 33.9 \log f - 13.82 \log h_B - a(h_m) + (44.9 - 6.55 \log h_B) \log d + C \quad (12)$$

Where,

- L = Median path loss in Decibels (dB)
- C=0 for medium cities and suburban areas
- C=3 for metropolitan areas
- f = Frequency of Transmission in Megahertz (MHz)(500MHz to 200MHz)
- $h_B$  = Base Station Transmitter height in Meters (30m to 100m)
- d = Distance between transmitter and receiver in Kilometers (km) (up to 20kilometers)
- $h_m$  = Mobile Station Antenna effective height in Meters (m) (1 to 10metres)
- $a(h_m)$  = Mobile station Antenna height correction factor as described in the Hata Model for Urban Areas.
- For urban areas,  $a(h_m) = 3.20(\log_{10}(11.75h_m))^2 - 4.97$ , for  $f > 400$  MHz
- For sub-urban and rural areas,  $a(h_R) = (1.1 \log(f) - 0.7)h_R - 1.56 \log(f) - 0.8$

## VI. MATERIALS AND METHODS

### A. Received Power Measurement

Received power readings were recorded from multiple Base Transceiver Stations (BTSs) situated within the rural terrain between the city of Jos and Keffi town, Nigeria. The instrument used was a Cellular Mobile Network Analyser (SAGEM OT 290) capable of measuring signal strength in decibel milliwatts (dBm). Received power ( $P_R$ ) readings were recorded within the 1800MHz frequency band at intervals of 0.1km away from the BTS. The Mobile Network Parameters obtained from the Network Provider (MTN - Nigeria) include the Mean Transmitter Height of 33 meters and Mean Effective Isotropic Radiated Power (EIRP) of 44dBm.

### B. Field strength Prediction Procedure

The procedure involved analyzing each BTS separately. During network training, validation and testing, field strength data recorded from a given BTS is randomly split as follows: 50% training, 10% validation and 40% testing.

### C. Statistical Indices for Performance Comparison

The performance comparison of predictors is based on the Root Mean Square Error (RMSE), given by (13), and the Coefficient of Determination ( $R^2$ ), given by (14). RMSE is essentially a measure of the differences between predicted and observed values. The smaller the RMSE, the higher the prediction accuracy of the model.  $R^2$  ranges between 0 and 1, but can be negative, which indicates the model is inappropriate for the data. A value closer to 1 indicates that a greater proportion of variance is accounted for by the model.

$$RMSE = \sqrt{\frac{\sum_{i=1}^N (M-P)^2}{N}} \quad (13)$$

Where,

M – Measured Path Loss  
P – Predicted Path Loss  
N- Number of paired values

$$R^2 = 1 - \frac{\sum_{i=1}^N (y_i - \hat{y}_i)^2}{\sum_{i=1}^N (y_i - \bar{y}_i)^2} \quad (14)$$

Where

$y_i$  is the measured path loss,  
 $\hat{y}_i$  is the predicted path loss and  
 $\bar{y}_i$  is the mean of the measured path loss values.

## VII. RESULTS AND ANALYSIS

Figs. 5 to 10 depict graphical performance comparisons of the predictors. The figures show that across the 6 Base Transceiver Stations, the



computational networks are convergent in terms of performance. The COST 231 Hata model on the other hand significantly underestimates the field strength on all but BTS 2. The disparity could stem from the fact that the terrain for which the model was formulated could have had higher clutter congestion than the one under investigation. Table 1 shows a

statistical performance comparison of the Predictors. The table shows that on the average, the most accurate of the predictors is the RBF-NN with the least RMSE value of 4.64dBm and the highest R<sup>2</sup> value of 0.84. Nevertheless, all three computational networks are recommended for field strength estimation across the terrain in question.

Table 1: Statistical Performance Comparison of Predictors

MODEL	STATS.	BST 1	BST 2	BST 3	BST 4	BST 5	BST 6	MEAN
RBF-NN	RMSE(dBm)	5.66	4.78	4.90	3.69	5.25	3.74	4.67
	R <sup>2</sup>	0.78	0.82	0.82	0.90	0.81	0.90	0.84
ANFIS	RMSE(dBm)	4.98	6.77	4.33	4.35	4.79	3.59	4.80
	R <sup>2</sup>	0.83	0.64	0.86	0.86	0.84	0.91	0.82
MLP-NN	RMSE(dBm)	4.70	6.95	4.26	4.65	6.57	4.30	5.24
	R <sup>2</sup>	0.85	0.62	0.86	0.84	0.71	0.87	0.79
COST 231 Hata	RMSE(dBm)	39.49	7.73	17.15	13.55	9.52	11.14	16.43
	R <sup>2</sup>	-0.24	0.63	-0.61	-0.12	0.54	0.40	0.10

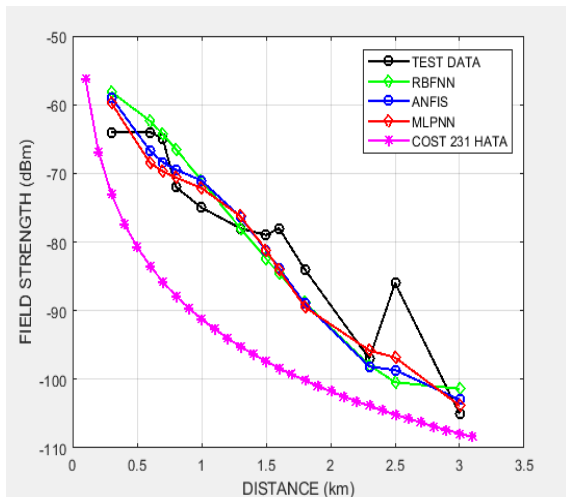


Fig. 5: Model Comparison for BTS 1

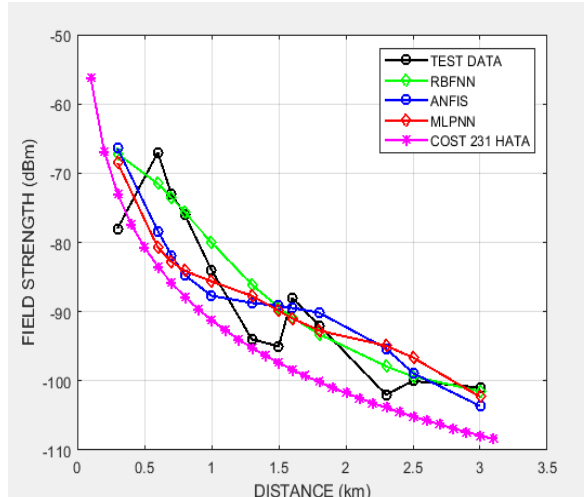


Fig. 6: Model Comparison for BTS 2

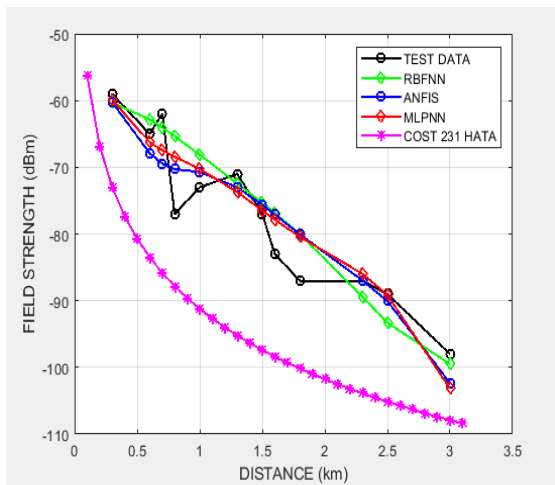


Fig. 7: Model Comparison for BTS 3

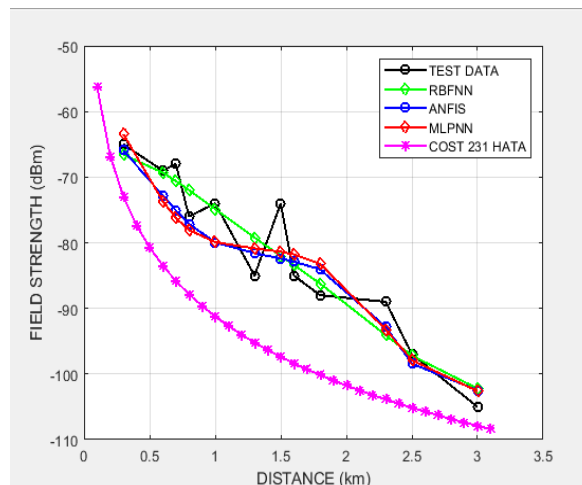


Fig. 8: Model Comparison for BTS 4

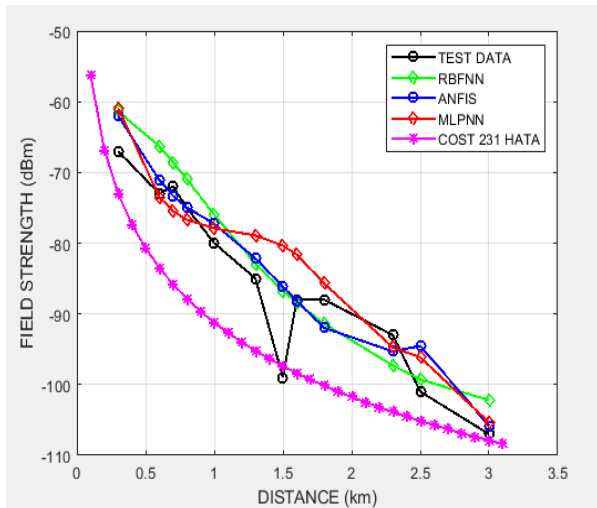


Fig. 9: Model Comparison for BTS 5

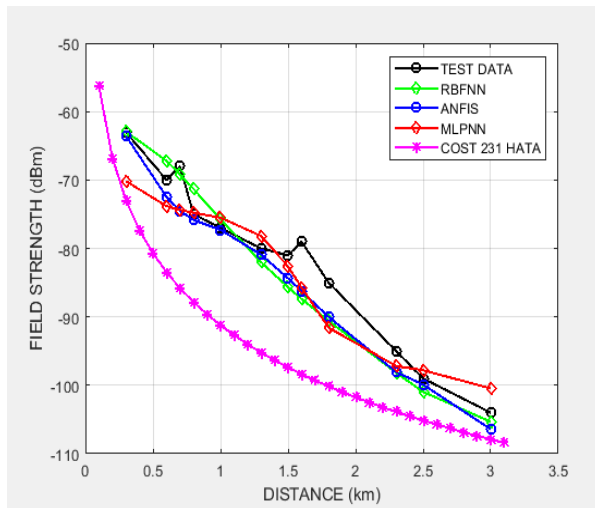


Fig. 10: Model Comparison for BTS 6

### VIII. CONCLUSION

This paper presents a computational approach to field strength determination across a typical Guinea Savanna rural terrain. The computational networks were trained, validated and tested with field strength data recorded at 1800MHz, from BTSs along the terrain. It was discovered that the computational networks have a combined average prediction RMSE value less than 5dBm, while the COST 231 Hata model underestimates the field strength. The most accurate predictor however, is the RBF-NN with a RMSE value of 4.67dBm.

### REFERENCES

- [1]. Sumit J. and Vishal G. A Review on Empirical Data Collection and Analysis of Bertoni's Model at 1.8 GHz. *International Journal of Computer Applications* (0975 – 8887) Volume 56, No.6, 2012, pp 17- 23.
- [2]. Athanasiadou G.E., Nix A.R., McGeehan J.P. „A Microcellular Ray-Tracing Propagation Model and Evaluation of its Narrowband and Wideband Predictions”, *IEEE Journal on Selected Areas in Communications, Wireless Communications series*, vol. 18, no 3, 2000, pp. 322-335.
- [3]. Popescu I., Nafori I., Gavrioloia G. Field Strength Prediction in Indoor Environment with a Neural Network Model:FACTA UNIVERSITATIS (NIS), Series: Electronics and Energetics. Vol. 14, No. 3, 2001, pp 329-336.
- [4]. Deme C. A. Development and Comparison of Artificial Neural Network Techniques for Mobile Network Field Strength Prediction across the Jos-Plateau, Nigeria. *Journal of Multidisciplinary Engineering Science and Technology (JMEST) ISSN: 2458-9403 Vol. 3 Issue 6, 2016, pp 1-7.*
- [5]. Anwasha B., Shounak D., Amit K., D. N. T. Development strategy of eye movement controlled rehabilitation aid using Electrooculogram. *International Journal of Scientific & Engineering Research*, Volume 3, Issue 6, June-2012, 1 ISSN 2229-5518. Pp 1-6.
- [6]. Popescu, I., Kanatas, A., Angelou, E., Naforita, I., & Constantinou, P. *Applications of generalized RBF-NN for path loss prediction*. 13th IEEE International Symposium on Personal, Indoor and Mobile Radio Communications (PIMRC 2002), 1, 2002, 484–488.
- [7]. Tsung-Ying S., Chan-Cheng L., Chung-Ling L., Shent-Ta H., Cheng-Sen H. A Radial Basis Function Neural Networks with Adaptive Structure via Particle Swarm Optimisation, 2014, pp.423-437
- [8]. Deme A.C. Field Strength Determination in a Tropical Metropolitan Environment Using Computational Intelligence Techniques. *American Journal of Engineering Research (AJER)* e-ISSN: 2320-0847 p-ISSN : 2320-0936 Volume-5, Issue-8, 2016, pp-276-284. www.ajer.org
- [9]. Jang J.S. Adaptive Network Based Fuzzy Inference System”, *IEEE Trans. On Systems*

- 
- [10] Man. and Cybernetics, Vol.23, No.3, 1993, pp 665-685
- [12] Jang J.S. Adaptive Network Based Fuzzy Inference System", IEEE Trans. On Systems Man. and Cybernetics, Vol.23, No.3, 1993, pp 665-685
- [10] Takagi T., Sugeno M., "Fuzzy identification of systems and its applications to modeling and control", IEEE Trans. on Systems, Man and Cybernetics, Vol. 15, No. 1, pp. 116-132, 1985.
- [13] Popescu I., Naforni I., Gavriloaia G. Field Strength Prediction in Indoor Environment with a Neural Network Model: *FACTA UNIVERSITATIS (NIS), Series: Electronics and Energetics*. Vol. 14, No. 3, 2001, pp 329-336.
- [11] Liang H., Zaiyi L., and Lian Z. Physical-Rules-Based Adaptive Neuro-Fuzzy Inferential Sensor Model for Predicting the Indoor Temperature in Heating Systems. Hindawi Publishing Corporation, *International Journal of Distributed Sensor Networks*. Volume 2012, Article ID 517826, 10 pages, pp 1-10.
- [14] Östlin, E., Zepernick, H.J., and Suzuki, H. Macrocell radio wave propagation prediction using an artificial neural network. IEEE Semiannual Vehicular Technology Conference, 1, 2004, pp 57–61.